International Information and Engineering Technology Association
Advancing the World of Information and Engineering

International Journal of Heat and Technology
Vol. 42, No. 6, December, 2024, pp. 1952-1962
Journal homepage: http://iieta.org/journals/ijht

Effect of Twist Ratios on Heat Transfer for Circular-Cut Twisted Tape Inserts in U-Shaped Pipe

Md. Moniruzzaman Bhuyan[1,2*], Mashky Chowdhury Surja[3], Ujjwal Kumar Deb[2]

[1] Department of Mathematics, Chittagong University of Engineering & Technology, Chittagong 1230, Bangladesh
[2] Department of Mathematics, International University of Business Agriculture and Technology, Dhaka 4349, Bangladesh
[3] School of Science, Engineering & Technology, East Delta University, Chittagong 4209, Bangladesh

Corresponding Author Email: mmbhuyan87@gmail.com

https://doi.org/10.18280/ijht.420612

Received: 7 July 2024
Revised: 11 September 2024
Accepted: 26 September 2024
Available online: 31 December 2024

Keywords:
circular-cut inserts, twist ratio, velocity, k-omega turbulent model, numerical simulation, heat transfer

ABSTRACT

To study the turbulent flow of fluid in circular-cut twisted tape inserts with inserts of varying twist ratios, a numerical simulation has been conducted. The heat transfer phenomenon of fluids in the tubular pipe is analysed with the help of a *k*-ω turbulent model. During the numerical simulation, study was conducted where the Reynolds numbers (Re) was kept in the range $3700 \leq Re \leq 23650$ under a constant temperature condition and twist ratios 3.0, 3.25, 3.5, 3.75, 4.0 and without insert separately. The length of the inserts is 800 mm on both sides with water as the working fluid. Numerical results show that the Wall Temperature, Bulk Temperature, effectiveness (ε), Nusselt number (Nu), the friction factor (f) and the thermal performance (η) show a downward trend with the twist ratio of the inserts. The vorticity exhibits a stable pattern in absence of inserts while demonstrating irregular pattern at cut-positions when there are circular-cut twisted tape inserts. The results also show that the heat transfer behavior depends not only on the difference in the geometrical shapes of the insert but also on their twist ratio. For the twist ratio 3, friction factor enhances 5.01-5.96 times compared to without insert and also the effectiveness improves 1.88 times. In case of thermal enhancement, its performance is 1.31-1.92 times better than without insert.

1. INTRODUCTION

Machine-driven devices are devices that are operated by machines or automated systems. Machine-driven devices are widely used in manufacturing and production industries to streamline the process, increase efficiency, and reduce costs [1]. These technologies are driving the growth of the 4IR (Fourth Industrial Revolution) which emphasizes the integration of digital and physical systems to create “smart devices” that are more efficient, flexible, and responsive to industrial demands. The heat transfer devices are related to heat exchangers, radiators, boilers, heat pumps, evaporators, condensers, heat sinks, etc. The exchange of heat can differ over time due to various factors including the geometrical shapes of the pipe, flow rate, temperature, pressure, and its inserts [2, 3]. In 2023, Khargotra, Rohit et al. found that the turbulance of the fluid in a corrugated tube Heat exchanger increases in the presence of the twisted tape turbulator. This improves the system’s efficiency by enhancing its thermal performance [4].

Mechanical engineers use a variety of tools and techniques to analyze and optimize heat transfer in their designs. Computational fluid dynamics (CFD) is a common tool used to model the flow of fluids and heat transfer within mechanical systems [5]. The ability of twisted tape inserts to create turbulence in the flow of fluid, resulting in the enhancement in heat transfer, makes them a popular choice in heat transfer applications [6]. This turbulence increases the rate of heat transfer between the fluid and the surrounding surface, leading to an improvement in performance and efficiency. The use of twisted tape inserts is a passive method of heat transfer enhancement, meaning that it does not require any external power or energy [7]. This makes it a practical solution which is also cost-effective for many industrial applications. Twisted tape inserts are also known for their consistency in performance and effectiveness.

Overall, twisted tape inserts are a popular and effective solutions for enhancing heat transfer in a variety of industrial applications. Inserts in a U-shaped pipe are typically used to enhance fluid flow and prevent turbulence [8]. The U-shaped pipe is often found in applications where the fluid needs to be transported from one point to another, such as in industrial or chemical processing plants. This insert is typically a metal coil that is inserted into the pipe, creating a spiral flow path for the fluid [9]. The spiral flow path helps to reduce turbulence and increase the velocity of the fluid, resulting in improved flow and reduced pressure drop [10, 11]. This insert is typically a series of flat plates or vanes that are placed inside the U-shaped pipe. Inserts can also be used to increase heat transfer in U-shaped pipes [12]. A circular-cut twisted tape insert can be used to enhance heat transfer by increasing the surface area of contact of the fluid inside the pipe which creates turbulence.

In 2011, Ahamed et al. [13] had experimentally compared the effect of perforation of twisted tape inserts on the heat transfer coefficient and effectiveness, which increase by 3.5 and 4.0 times for the twist ratio of 4.55.

In 2013, Salam et al. [14] and 2015 Hossain et al. [15] conducted an experimental study on heat transfer in a round tube provided with a twisted tape insert of twist ratio 5.5 consisting of rectangular-cut inserts. The heat transfer rate improves 1.9 to 2.3 times in comparison to a tube without insert. The numerical investigation by Acherjee et al. [16] on heat transfer enhancement in pipe flow with perforated inserts showed how the heat transfer in pipe flow is affected by the angle of perforation on inserts. They found that when the perforation angle is set at 65°, the Nusselt number is higher and the thermal performance evaluation criterion (PEC) shows better results compared to other angles. Higher Reynolds numbers result in a decrease in fluid temperature, indicating improved heat transfer up to a certain point.

Simulations by Chowdhury et al. [17] show that a plain insert with a twist ratio of 3.5 yields better heat transfer rates compared to inserts of other twist ratios. The twist ratio is defined as the ratio of the pitch of the tape insert to its width. A plain twist ratio of 3.5 means that the pitch of the tape is 3.5 times its width. As the Reynolds number increases from 5000 to 25,000, the rate of heat transfer improves. The Reynolds number represents the pattern of the fluid flow, with higher values indicating more turbulent flow. The Nusselt number, which is a dimensionless measure of heat transfer, also increases with the Reynolds number in the same scenario, suggesting enhanced convective heat transfer.

In 2023, Nashee's [18] numerical study on the flow and heat transfer characteristics of the fluid in a corrugating channel showed that the increase in the Reynold's number resulted in an increase in the mean Nusselt number for all cases of the corrugated channel. In the numerical study conducted by Nashee et al. [19] of the flow of fluid in vertical rectangular channels consisting of three different obstacle shapes in 2024, it was found that the largest increase in pressure and friction factor were observed in case of a triangular obstacle, which yielded in a better heat transfer compared to semi-circular or rectangular obstacles at the cost of a large pressure differential. In 2023, Shakir's [20] study predicted the boiling flow of heat transfer in an array of inline micro-pin-fins heat sink where the simulation results were found to be approximately similar to real lab tests. In a rectangular channel with triangular obstacles of three different heights (4 µm, 6 µm and 8 µm), Hamood et al. [21] found that the largest value of heat transfer is obtained for an obstacle height of 8µm.

In 2024, Nashee [22] conducted a numerical simulation to explore the relationship between the Reynolds number, the cutting ratio, and the thermal performance in a specific cutting type. Here's a summary and interpretation of her findings: Lower Reynolds numbers generally lead to higher thermal performance efficiency. A higher cutting ratio improves thermal performance, with the double cut type showing superior results compared to the single cut type. The optimal configuration for thermal performance in this study was found with the double cut type and a cutting ratio of 0.9, especially effective at a Reynolds number of 5000.

This paper investigates the effect of various twist ratios of circular-cut twisted tape inserts on the heat transfer by a fluid in a U-shaped circular pipe. Keeping the Reynolds number in the interval of 3700-23610, the study focuses on turbulent flow regimes. The simulation utilizes the Finite Element Method (FEM) to model the non-isothermal *k*-*ω* turbulent flow within the pipe under constant temperature conditions. The objective is to analyze how different twist ratios of the circular cut twisted tapes influence heat transfer efficiency. The study examines how different twist ratios affect heat transfer. This is crucial as the twist ratio influences the enhancement of turbulence and mixing within the pipe, thereby affecting heat transfer.

2. GOVERNING EQUATIONS

To calculate the fluid dynamical performance inside the U-loop pipe, CFD is the most reliable method for a wide range of applications. By means of computer and numerical methods, CFD resolves problems involving the flow of fluid inside the tube And CFD procedure solves the Navier-Stokes equation where the mesh is generated by using the FEM [23]. The fundamental governing equations of fluid dynamics, which form the basis of CFD, are the Equation of continuity, momentum and energy [24].

$$\frac{\partial \rho}{\partial t} + \nabla \cdot (\rho \mathbf{u}) = 0 \tag{1}$$

$$\begin{aligned} \rho(\mathbf{u}\cdot\nabla)\mathbf{u} &= \nabla\cdot[-pI + (\mu+\mu_T)(\nabla\mathbf{u} + (\nabla\mathbf{u})^T) \\ &\quad -\frac{2}{3}(\mu+\mu_T)(\nabla\cdot\mathbf{u})I - \frac{2}{3}\rho KI] + F \end{aligned} \tag{2}$$

Menter [25] derived the *k*-ω turbulent model which solves the turbulence of the kinetic energy, *k*, of fluids where ω is the dissipation rate of turbulent kinetic energy which is commonly known as the specific dissipation rate. The CFD Module has the *k*-ω model revised by Wilcox [26].

$$\rho(\mathbf{u}\cdot\nabla)k = \nabla\cdot[(\mu+\mu_T\sigma_k^{*})\nabla_K] + p_k - \rho\beta^{*}\mathrm{k}\omega \tag{3}$$

$$\rho(\mathbf{u}\cdot\nabla)\omega = \nabla\cdot[(\mu+\mu_T\sigma_\omega)\nabla\omega] + \alpha\frac{\omega}{\mathrm{k}}\mathrm{P_k} \text{ -}\rho\beta\omega^2 \tag{4}$$

In this model ω is an inverse time scale that is associated with the turbulence flow. The most advantage of the *k-ω* model is that it may applied throughout the boundary layer without further improvement. The turbulent viscosity (μ_T) is calculated as follows:

$$\mu_{\mathrm{T}} = \rho\frac{\mathrm{K}}{\omega} \tag{5}$$

$$P_k = \mu_T\left[\nabla\mathbf{u}:(\nabla\mathbf{u}) + (\nabla\mathbf{u})^T - \frac{2}{3}(\nabla\cdot\mathbf{u})^2\right] - \frac{2}{3}\rho k\nabla\cdot\mathbf{u} \tag{6}$$

Equation of energy is as follows:

$$\rho C_p\frac{\partial T}{\partial t} + \rho C_p\mathbf{u}\cdot\nabla T = \nabla\cdot(k\nabla T) + \mathbf{Q} \tag{7}$$

If the fluid is initially at rest, i.e., $\mathbf{u}$ = 0, Eq. (7) can be written as:

$$\rho C_p \frac{\partial T}{\partial t} + \nabla \cdot (-k\nabla T) = \mathbf{Q} \quad (8)$$

The convective heat transfer coefficient, h, is calculated using:

$$h = \frac{\mathbf{Q}}{T_w - T_b} \quad (9)$$

where, the bulk temperature is defined as the average of the inlet and outlet temperatures of the fluid in the tube.

In the study of Bhuiya et al. [27], the effectiveness of the insert in the tube is calculated by:

$$\varepsilon = \frac{T_o - T_i}{T_{wav} - T_i} \quad (10)$$

where, T_o, T_i and T_{wav} are outlet temperature, Inlet temperature and Wall average temperature respectively.

The Nusselt number of the fluid is evaluated using:

$$Nu = \frac{hD}{k} \quad (11)$$

where, k is the fluid's thermal conductivity and D is the diameter of the tube's cross section.

In the literature of Bhuiya et al. [28], the pressure drop of the fluid from inlet to outlet, ΔP, and friction factor f are calculated by Darcy method.

$$\Delta P = h\rho g \quad (12)$$

where, h is the head loss of the fluid, which is calculated using:

$$h = \frac{flu^2}{2gD} \quad (13)$$

Finally we have Eq. (14) using Eqs. (12) and (13).

$$\Delta p = \frac{l}{D} \cdot \frac{fu^2\rho}{2} \quad (14)$$

The thermal enhancement efficiency, η, is calculated using [28, 29]:

$$\eta = \frac{Nu_t}{Nu_p} \quad (15)$$

2.1 Boundary conditions

The boundary conditions are aligned with the k-ω model by Wilcox [26], i.e.:

$$\mathbf{u} = -\mathbf{u}_0 \mathbf{n} \quad (16)$$

$$k = \frac{3}{2}\left(\mathbf{u}_0 I_T\right)^2 \quad (17)$$

$$\omega = \frac{k^{\frac{1}{2}}}{\left(\beta_0^*\right)^{\frac{1}{4}} L_T} \quad (18)$$

Setting the initial inlet temperature of the fluid, T_{in}, equal to *293.15K*, the no sleep wall functions condition are assumed by:

$$\mathbf{u} \cdot \mathbf{n} = 0 \quad (19)$$

$$[(\mu + \mu_T)(\nabla \mathbf{u} + (\nabla \mathbf{u})^T) - \frac{2}{3}(\mu + \mu_T)(\nabla \cdot \mathbf{u})I - \frac{2}{3}\rho k I]\mathbf{n} = -\rho \frac{u_\tau}{\delta_w} \mathbf{u}_{\tan g} \quad (20)$$

$$\mathbf{u}_{\tan g} = \mathbf{u} - (\mathbf{u} \cdot \mathbf{n})\mathbf{n} \quad (21)$$

$$\nabla k \cdot \mathbf{n} = 0, \omega = -\rho \frac{c_\mu K^2}{K_v \delta_w \mu} \quad (22)$$

The inner wall of the tube and the wall function of the outlet domain are governed by the following equations.

$$[-pI + (\mu + \mu_T)(\nabla \mathbf{u} + (\nabla \mathbf{u})^T) - \frac{2}{3}(\mu + \mu_T)(\nabla \cdot \mathbf{u})I - \frac{2}{3}\rho k I] = -f_0 \mathbf{n} \quad (23)$$

$$\nabla k \cdot \mathbf{n} = 0 \quad (24)$$

$$\nabla \omega \cdot \mathbf{n} = 0 \quad (25)$$

The constant temperature conditions of the boundary of the domain applied by:

$$T = T_o = 500\text{K} \quad (26)$$

3. COMPUTATIONAL DOMAIN SETUP AND MESH DESIGN

Figure 1. Computational full domain

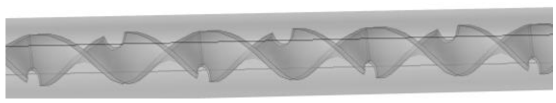

Figure 2. Computational full inserts domain

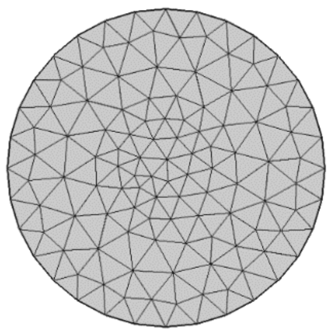

Figure 3. Computational inlet mesh design

Table 1. Distinct mesh elements comparison

Properties	Ratios					
	3	**3.25**	**3.5**	**3.75**	**4.0**	**No Insert**
Tetrahedral elements	98901	102272	172534	263232	151549	50273
Triangular elements	24642	24670	24950	36894	27524	12842
Elements of edge	3238	3194	4367	4792	3583	764
Elements of vertex	224	208	368	214	216	12
Elements quality	0.067	0.08103	1.053E-9	1.355E-6	0.01592	0.2337
Average element	0.7024	0.7105	0.5804	0.695	0.6862	0.7445

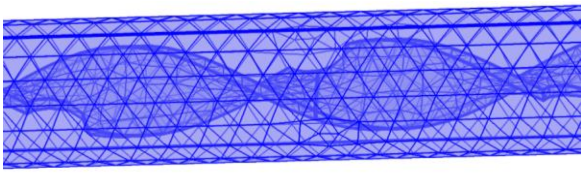

Figure 4. Computational mesh design for inserts

Figure 1 shows a computational domain for the twist ratio 3.0. A modified U-loop circular-cut twisted tape insert has been considered, with a pipe length of 1855 mm, inner diameter of 26 mm, thickness of 2 mm and circular cut radius of 5 mm. Computational simulations mesh design have been performed to adjust until the desired outcomes obtained accurately. For large domain, computer processor is an important issue that's why fine mesh is considered for the whole domain. Simulation has been performed on a high-performance computer whose configuration is 16GB DDR3 RAM and Intel core i7 processor. COMSOL MULTIPHYSICS is used for the numerical simulations, which is a software based on Finite Element Method [23, 24]. The computational full-length inserts domain is shown in Figure 2 and the inlet mesh is represented in Figure 3. Near the insert positions, the Mesh element becomes more complex, as shown in Figure 4. The comparison between various meshes is shown in Table 1.

4. NUMERICAL RESULTS DISCUSSION

Computational simulations have been performed with FEM, which uses tetrahedral elements for complex geometries. The primary purpose of the numerical simulation model is to observe the amount of heat transfer enhancement in a U-shaped pipe. The k-ω non-isothermal turbulent flow model is taken into consideration due to the geometrical shape of the insert. The steady of time has been taken for the simulation. Tube thickness is neglected for this numerical analysis. In this U-loop tubular pipe water has been taken as the employed fluid. To understand the effect of twist ratio in the heat transfer phenomenon, numerical simulations have been carried out using twisted tape inserts of various twist ratios such as 3.0, 3.25, 3.5, 3.75, and 4.0.

4.1 Temperature distribution for without insert

Figures 5(a)-(h) show the simulation results of temperature distribution without insert. Initially the input temperature 293.15K in the inlet of the pipe domain. It is also observed that the outlet temperature is 324.01K, where the Reynolds number is 3700 in the position of 0.75m from the inlet. If the Reynolds number is increased gradually to 6360, 9020, 11680, 14340, 17000, 19660 and 22320 where the maximum temperatures obtained were 318.24K, 315.84K, 314.46K, 313.5K, 312.76K, 312.16K, and 311.67K respectively. From observation of the numerical simulation, it is found that the outlet temperature is decreased where the Reynolds number is increased [29, 30].

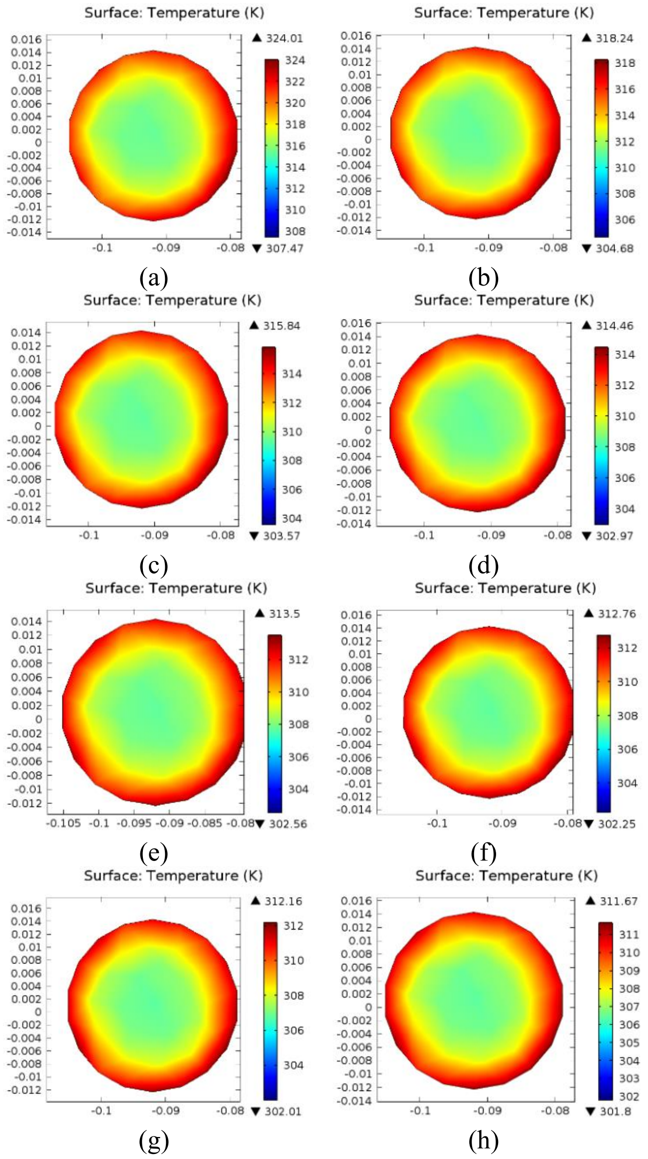

Figure 5. Temperature magnitude without insert

4.2 Temperature distribution for twist ratio 3.0

Figures 6(a)-(h) represent the simulation results for the twist ratio 3.0. Initially the input temperature is 293.15K in the inlet. It is also observed that the outlet temperature is 334.93K, where the Reynolds number is 3700 in the position of 0.75 m from the inlet. If the Reynolds number is increased gradually to 6360, 9020, 11680, 14340, 17000, 19660 and 22320 where the maximum temperatures obtained were 330.27K, 329.14K, 328.54K, 328.14K, 327.82K, 327.56K, and 327.34K respectively. From the observation of the numerical simulation, it is found that the outlet temperature is decreased where the Reynolds number is increased [29, 30].

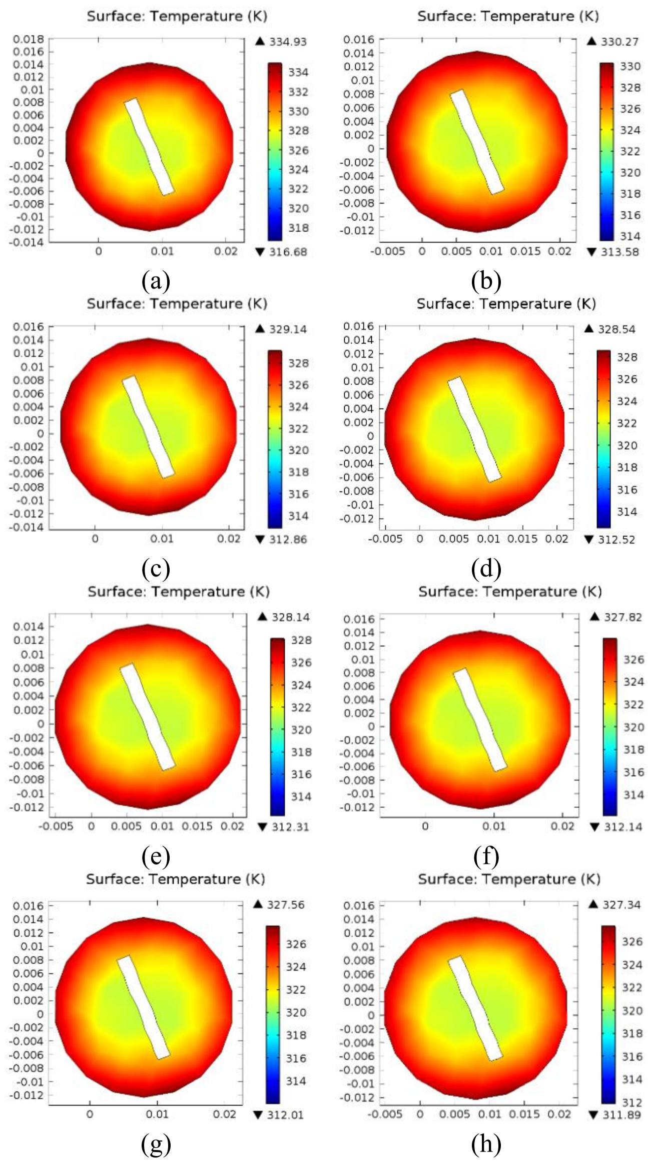

Figure 6. Temperature magnitude for with insert of twist ratio 3.0

4.3 Wall temperature

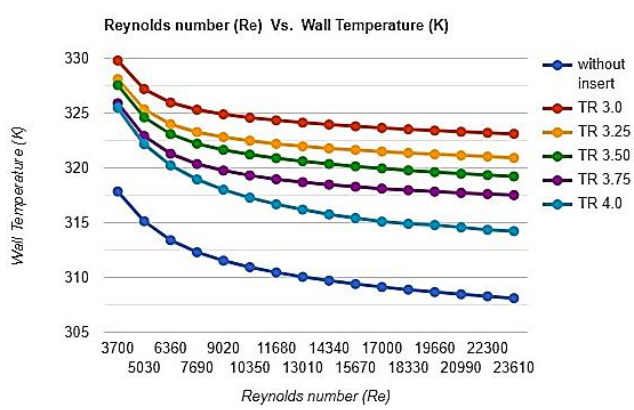

Figure 7. Reynolds number vs. wall temperature

The heat transfer phenomena is investigated for circular-cut twisted tape inserts of various twist ratios (3, 3.25, 3.5, 3.75, and 4.0) as well as without insert. The results are illustrated in Figure 7, which shows the wall temperature variation with increasing Reynolds numbers for circular-cut twisted tape inserts with several twist ratios. For the one with a twist ratio of 3, a gradual decrease in wall temperature with an increase in Reynolds number is observed. A similar pattern was noted for the twist ratios 3.25, 3.5, 3.75, 4.0, and without insert, although the patterns varied slightly. For any studied Reynolds number, the tube equipped with an insert of twist ratio 3 has a higher wall temperature compared to others. It appears that a twist ratio of 3 is optimal, achieving the maximum heat transfer enhancement [16, 27-30].

4.4 Bulk temperature

Similarly, the bulk temperature variation with increasing Reynolds numbers for the circular-cut twisted tape inserts of same twist ratios: 3, 3.25, 3.5, 3.75, and 4.0, and without insert is studied. The results are depicted in Figure 8. For the twist ratio of 3, a gradual decrease in bulk temperature was observed with an increase in Reynolds number. This pattern remains consistent across all other ratios and without insert. The tube with an insert of twist ratio 3 has a higher bulk temperature compared to others for any studied Reynolds number. This indicates that an insert of twist ratio 3 provides the most efficient heat transfer [16, 27-30].

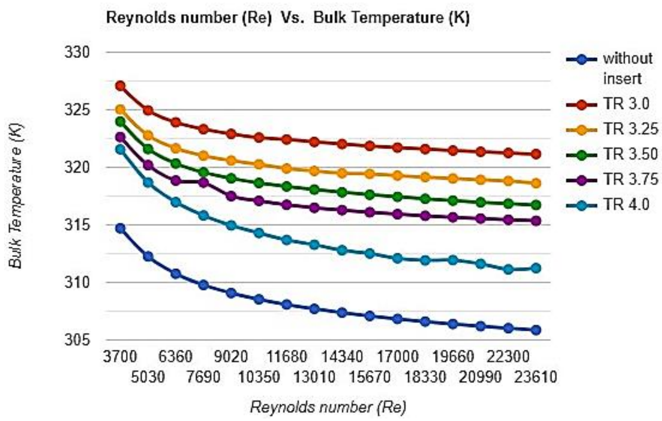

Figure 8. Reynolds number vs. bulk temperature

4.5 Effectiveness distribution

Figure 9 illustrates the effectiveness of heat transfer from one fluid to another. Higher effectiveness means more efficient heat transfer. The Figure 9 indicates a maximum enhancement of 1.88 folds. This implies that the heat transfer effectiveness of the fluid in the tube with an insert is 1.88 times higher compared to a plain tube under constant temperature conditions. In summary, using a twisted tape insert in a tube significantly enhances heat transfer effectiveness compared to twist ratios like 3.0, 3.25, 3.50, 3.75, 4.0 and a plain tube. The maximum enhancement (1.88 folds) occurs when the twist ratio of the circular-cut twisted tape insert is 3. This enhancement is caused by the circular-cut twisted tape insert which increases turbulence and improves mixing, which enhances the heat flow between the fluid inside the U-loop tubular pipe and the surrounding medium [29].

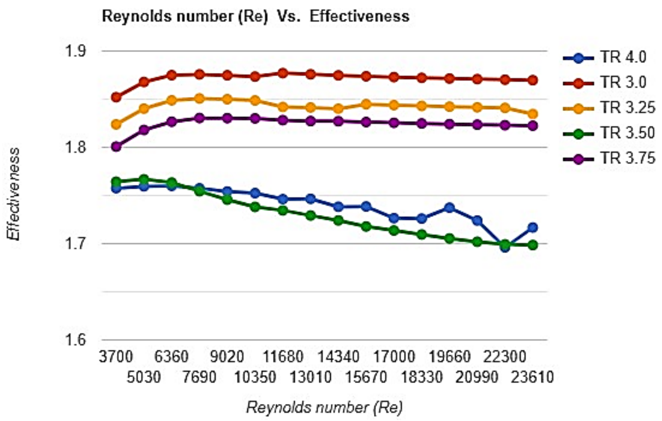

Figure 9. Reynolds number vs. effectiveness

4.6 Nu distribution

The relationship between Nu and Re is represented in Figure 10. It is observed that the Nusselt number and the Reynolds number show upward trend for circular-cut twisted tape inserts with all twist ratios studied. Figure 10 also highlights that smaller twist ratios result in better Nusselt numbers, indicating better turbulent intensity, resulting in an improved heat transfer. The numerical simulation results demonstrate that the tube with an insert of twist ratio 3.0 provides a higher Nusselt number than the inserts of other ratios and without insert [30-35].

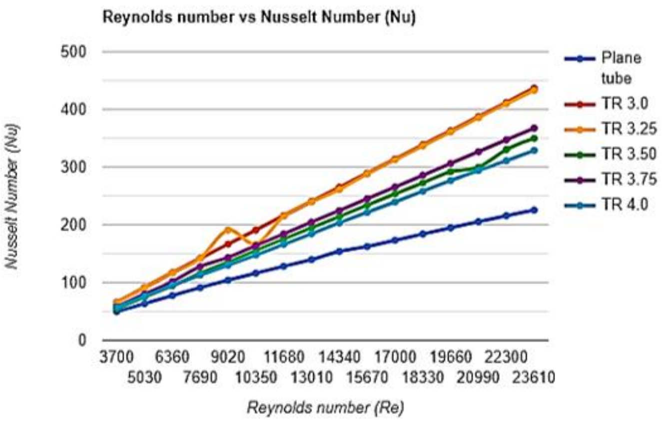

Figure 10. Reynolds number vs. Nusselt number

4.7 Friction factor distribution

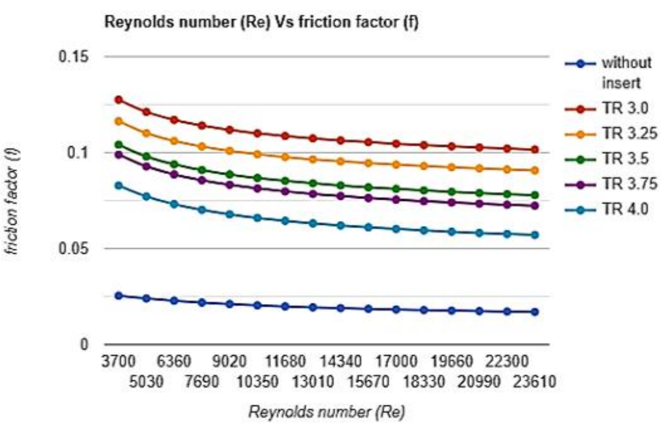

(a)

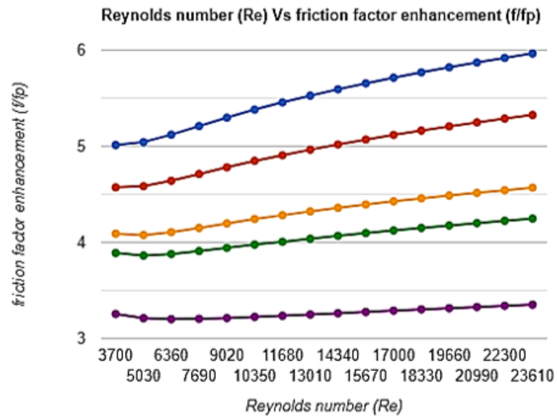

(b)

Figure 11. (a) Reynolds number vs. friction factor; (b) Reynolds number vs. friction factor enhancement index

Figure 11(a) shows the simulation results for twist ratios of 3.0, 3.25, 3.5, 3.75, 4.0, and without insert. The variations of friction factor (f) with Re, and the friction factor enhancement index (f/fp) with Reynolds number are shown in Figures 11(a) and 11(b) respectively. The numerical simulations indicate that the friction factor shows a downward trend while the friction factor enhancement index shows an upward trend with increasing Re across all cases. The twist ratio of 3.0 is more effective than other ratios and the condition without insert. Figure 11(b) shows, for Reynolds numbers ranging from 3700 to 23650, the friction factor values in tubes with twist ratios of 3.0, 3.25, 3.5, 3.75, and 4.0 were 5.96-5.01, 5.32-4.57, 4.56-4.09, 4.24-3.88, and 3.35-3.25 times higher, respectively, than those obtained for without insert [28, 33].

4.8 Thermal enhancement performance

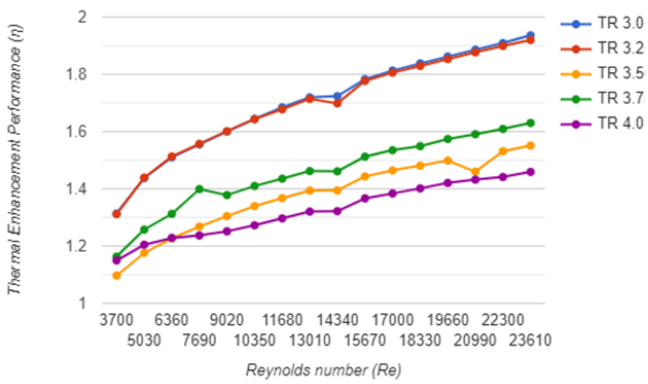

Figure 12. Thermal enhancement performance

For the enhancement method to be considered effective, the thermal enhancement performance should be greater than unity. Specifically, it suggests that the enhancement has a positive impact on heat transfer, making the system more effective compared to the baseline or reference system. The thermal enhancement performance of tubes fitted with circular-cut twisted tape inserts of various twist ratios, as obtained from numerical simulations, is depicted in Figure 12. The thermal enhancement performance rises for Reynolds number from 3700 to 13010, but exhibits different behaviors for Reynolds numbers from 14340 to 15670 and again from 17000 to 23650. The twist ratio of 3.5 showed an upward trend except at Reynolds number 20990. Tubes equipped with inserts of twist ratio 3.0 perform better in case of heat transfer compared to tubes with circular-cut twisted tape inserts of various twist ratios (3.25, 3.5, 3.75, and 4.0). For the studied Reynolds number range, tubes equipped with circular cut twisted tape inserts resulted in a better thermal performance than tubes without inserts by 1.31-1.92 times [28, 31-33].

4.9 Vorticity of the without insert pipe domain

Figures 13(a)-(p) represent the simulation results of the vorticity without insert pipe domain. It has been seen that in the position of 600 mm the vorticity magnitude is 6.8027(1/s). It is carried out for the Reynolds number is 3700. If the observed position is changed gradually from 620mm to 860 mm with an interval of 20 mm and from 860 mm to 880 mm with an interval of 10 mm, where the maximum vorticity is obtained at 7.4508(1/s), 6.7124(1/s), 7.5547(1/s), 7.425(1/s), 6.8363(1/s), 7.3122(1/s), 7.1664(1/s), 7.2569(1/s), 7.1503(1/s), 7.8997(1/s), 11.045(1/s), 10.844(1/s), 10.008(1/s), 8.105(1/s), and 7.1855(1/s) respectively. From the observation of the numerical simulation, it is found that when the Reynolds number is increased where the vorticity magnitude is fluctuating [34, 35].

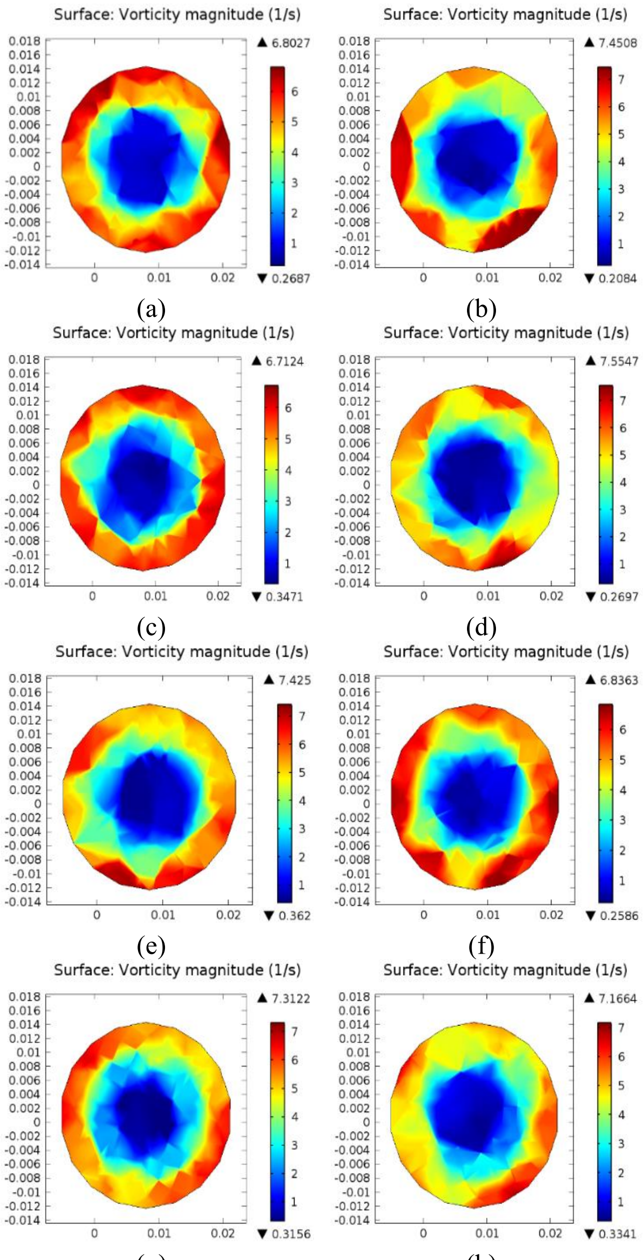

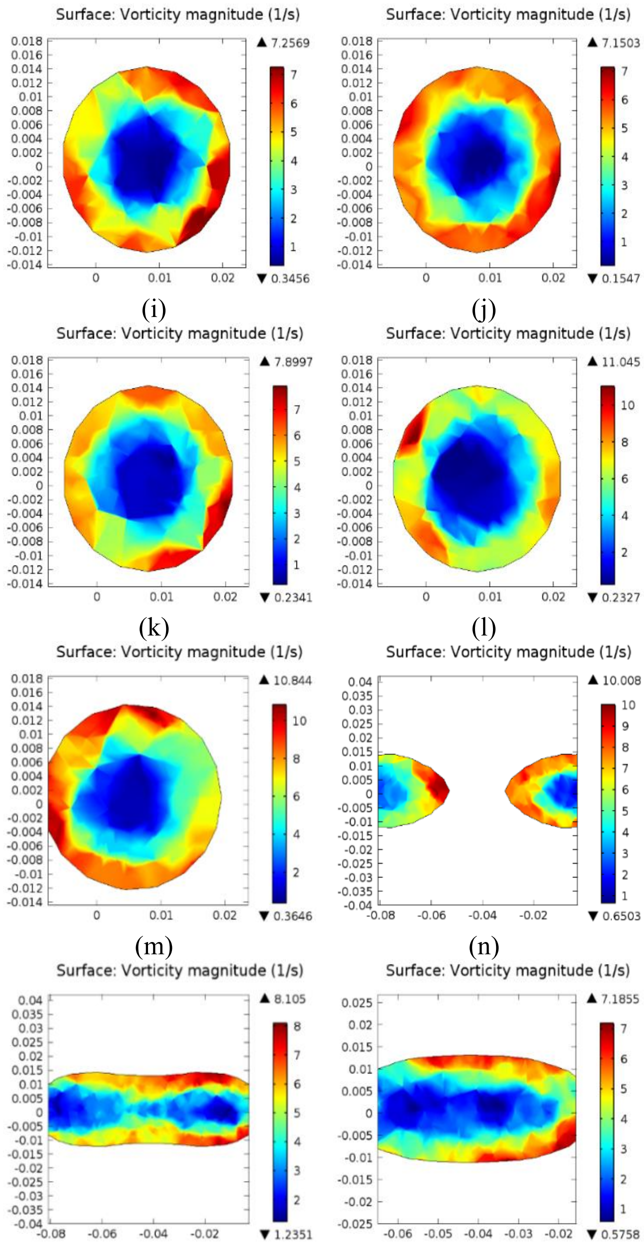

Figure 13. Vorticity magnitude at different positions without insert

4.10 Vorticity magnitude description with insert of twist ratio 3.0

Figures 14(a)-(p) represent the simulation results of vorticity for the twist ratio of 3.0. It has been seen that in the position of 600 mm the vorticity magnitude is 18.499(1/s). It is carried out for the Reynolds number of 3700. If the observed position is changed gradually from 620 mm to 860 mm with an interval of 20 mm and from 860 mm to 880 mm with an interval of 10 mm, the maximum vorticity obtained is 77.755(1/s), 23.702(1/s), 24.206(1/s), 40.898(1/s), 20.022(1/s), 48.128(1/s), 21.531(1/s), 42.694(1/s), 26.034(1/s), 91.395(1/s), 12.307(1/s), 11.12(1/s), 8.9588(1/s), 7.989(1/s), and 6.0698(1/s) respectively. From the observation of the numerical simulation, it is found that when the Reynolds number is increased the voracity magnitude is fluctuating [23, 24]. Vorticity magnitude increases drastically in the cut position of the inserts. This means the circular cut have the effect to enhance the heat transfer phenomena.

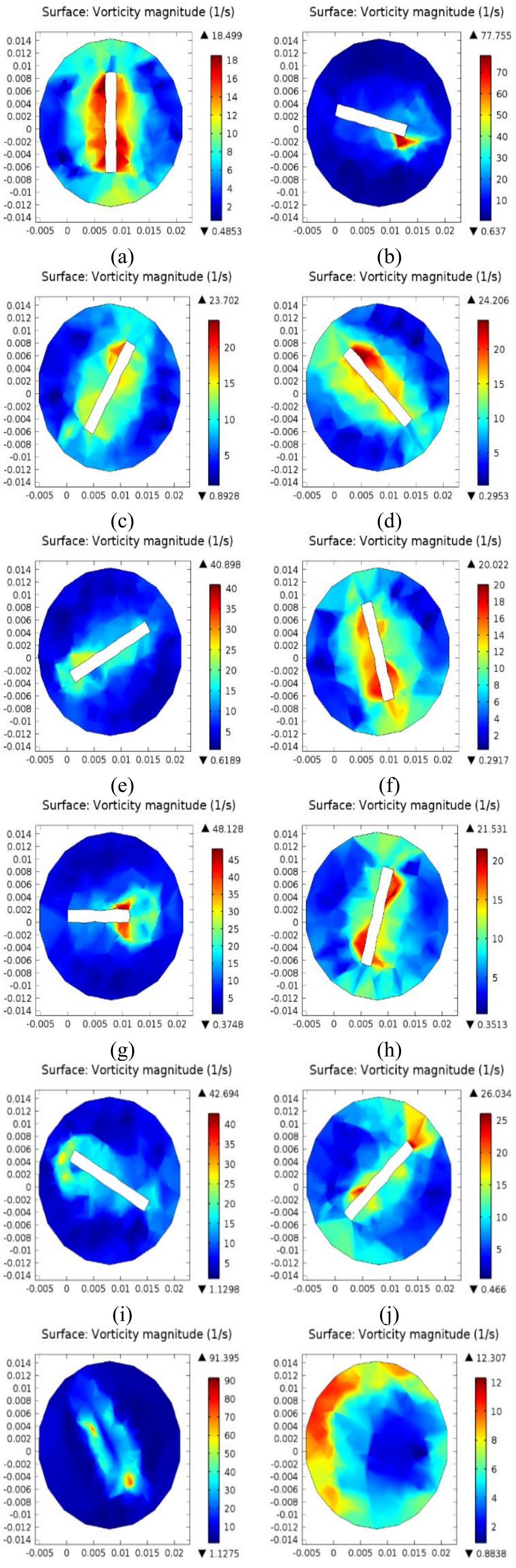

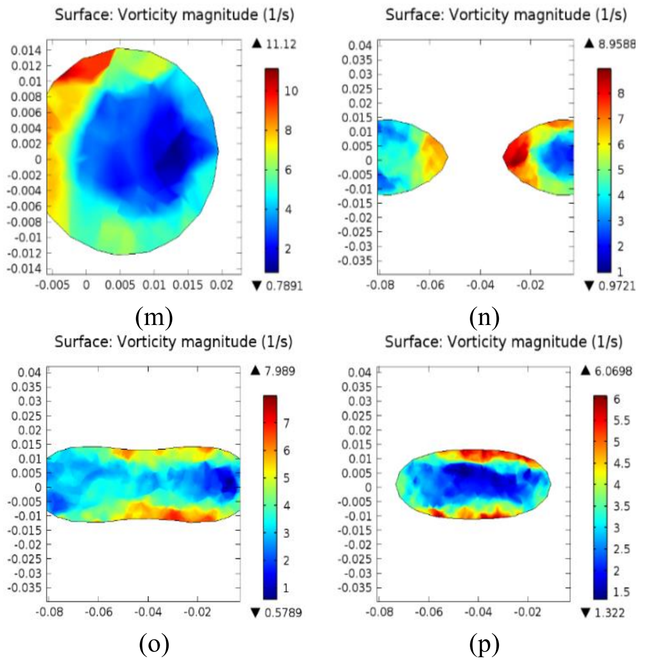

Figure 14. Vorticity magnitude at different positions with insert of twist ratio 3

5. CONCLUSIONS

Numerical simulations have been performed to analyse the heat transfer phenomenon of fluids flowing through tubes fitted with circular-cut twisted tape inserts of various twist ratios. The effect of twist ratios of circular-cut twisted tape insert (3.0, 3.25, 3.50 3.75, and 4.0) have been considered for the numerical simulations with constant temperature conditions and inserts length ranging from 600-880mm. On the basis of results obtained from numerical analysis, the following conclusions can be summarized:

(i) The wall temperature gradually decreases with increasing Reynolds number for the circular-cut twisted tape inserts with various twist ratios and without insert. For any studied Reynolds number, the tube with insert of twist ratio 3 has a higher wall temperature compared to others. It appears that a twist ratio of 3 is optimal, achieving the maximum heat transfer enhancement.

(ii) A bulk temperature gradually decreases with increasing Reynolds number for the circular-cut twisted tape inserts with various twist ratios and without insert. For the insert of twist ratio 3, a higher bulk temperature is observed compared to others for any studied Reynolds number, suggesting that an insert of twist ratio 3 provides a more efficient heat transfer compared to others.

(iii) The initial temperature is 293.15K whereas the outlet temperature is observed at 334.93K for the Reynolds number 3700. Increasing the Reynolds number gradually to 6360, 9020, 11680, 14340, 17000, 19660, and 22320, the maximum temperature was obtained at 330.27K, 329.14K, 328.54K, 328.14K, 327.82K, 327.56K, and 327.34K respectively. It can be deduced that the Reynolds number increases whereas the final temperature decreases for a constant temperature condition.

(iv) The heat transfer effectiveness of the fluid in the tube with circular-cut twisted tape inserts of various twist ratios is higher compared to the plain tube under constant temperature conditions. The maximum enhancement of 1.88 folds occurs when the twist ratio of the insert is 3.

(v) It is also deduced that with an increased of Nusselt number, temperature is decreased for inserts of various twist ratios (3.0 3.25, 3.5, 3.75, 4) and without insert.

(vi) The numerical simulations indicate that the friction factor shows a downward trend while the friction factor enhancement index shows an upward trend with increasing Reynolds number (Re) across all cases. The twist ratio of 3.0 is more effective than other ratios and the condition without insert. For Reynolds numbers ranging from 3700 to 23650, the friction factor values in tubes with twist ratios of 3.0, 3.25, 3.5, 3.75, and 4.0 were 5.96-5.01, 5.32-4.57, 4.56-4.09, 4.24-3.88, and 3.35-3.25 times higher, respectively, than those obtained for without insert.

(vii) Thermal performance factor tends to increase with decreasing twist ratio of circular-cut twisted tape inserts. For the studied range, the tube with a circular-cut twist ratio 3.0 yielded a higher thermal performance factor, 1.31-1.92 times, for Reynolds number of 3700-23650, compared to other twist ratios.

(viii) It has been seen that in the position of 600mm the vorticity magnitude is 18.499(1/s). It is carried out for the Reynolds number is 3700. If the observed position is changed gradually from 620 mm to 860 mm with an interval of 20 mm and from 860 mm to 880 mm with an interval of 10 mm, the maximum vorticity obtained is 77.755(1/s), 23.702(1/s), 24.206(1/s), 40.898(1/s), 20.022(1/s), 48.128(1/s), 21.531(1/s), 42.694(1/s), 26.034(1/s), 91.395(1/s), 12.307(1/s), 11.12(1/s), 8.9588(1/s), 7.989(1/s), and 6.0698(1/s) respectively. With insert and cut present in the insert length ranging from 600-800 mm, maximum vorticity is obtained at cut positions. Maximum vorticity reduces after 800 mm due to the absence of inserts. From the observation of the numerical simulation, it is found that the vorticity is fluctuating when the Reynolds number increases.

The results in this paper are obtained from FEM based numerical simulations. The experimental study will give a better understanding when compared to the numerical simulation results. Future work may include the experimental study and its comparison with the current results.

ACKNOWLEDGEMENT

The authors would like to express their sincere gratitude to the Centre of Excellence in Mathematics (CEM), Department of Mathematics, Mahidol University (MU), Bangkok-10400, Thailand, for their valuable technical support. We also extend our heartfelt thanks to the Simulation Lab, Department of Mathematics in the Faculty of Science and Technology, Chittagong University of Engineering and Technology (CUET), Chittagong-4349, for their assistance.

REFERENCES

[1] Huber, C., Rosentritt, M., Strasser, T., Behr, M. (2021). Machine-driven simulation of removing luting agent remnants from implant surfaces: An investigator-independent assessment of cleaning protocols. Journal of the Mechanical Behavior of Biomedical Materials, 121: 104584. https://doi.org/10.1016/j.jmbbm.2021.104584

[2] Penprase, B.E. (2018). The fourth industrial revolution and higher education. Higher Education in the Era of the Fourth Industrial Revolution, 10(1): 978-981. https://doi.org/10.1007/978-981-13-0194-0_9

[3] Uleanya, C. (2023). Scholarly discourse of the fourth industrial revolution (4IR) and education in Botswana: A scoping review. Education and Information Technologies, 28(3): 3249-3265. https://doi.org/10.1007/s10639-022-11298-9

[4] Khargotra, R., Kumar, R., Nadda, R., Dhingra, S., Alam, T., Dobrota, D., Chicea, A.L., András, K., Singh, T. (2023). A review of different twisted tape configurations used in heat exchanger and their impact on thermal performance of the system. Heliyon, 9(6): e16390. https://doi.org/10.1016/j.heliyon.2023.e16390

[5] Wagner, S. (2003). Computational fluid dynamics (CFD). High Performance Computing in Science and Engineering'02: Transactions of the High Performance Computing Center Stuttgart (HLRS), Springer, Berlin, Heidelberg. https://doi.org/10.1007/978-3-642-59686-5_20

[6] Al-Obaidi, A.R. (2023). The influence of different twisted tape inserts configurations on thermo-hydraulic performance and enhancement of heat transfer in the 3D circular tube. Korean Journal of Chemical Engineering, 40(4): 770-790. https://doi.org/10.1007/s11814-022-1342-6

[7] Dehankar, P.B., Joshi, K., Bhosale, V.A., Mulik, R.N. (2022). Assessment of twist tape thermal performance in heat transfer passive augmentation technique. Beni-Suef University Journal of Basic and Applied Sciences, 11(1): 29. https://doi.org/10.1186/s43088-022-00208-0

[8] Haque, M.R., Rahman, A. (2020). Numerical investigation of convective heat transfer characteristics of circular and oval tube banks with vortex generators. Journal of Mechanical Science and Technology, 34(1): 457-467. https://doi.org/10.1007/s12206-019-1044-0

[9] Faridi Khouzestani, R., Ghafouri, A. (2020). Numerical study on heat transfer and nanofluid flow in pipes fitted with different dimpled spiral center plate. SN Applied Sciences, 2(2): 298. https://doi.org/10.1007/s42452-020-2084-x

[10] Eiamsa-ard, P., Wongcharee, K., Kunnarak, K., Kumar, M., Eiamsa-ard, S., Pimsarn, M. (2022). Heat transfer characteristics of a swirling impinging air jet emerging from a triple spiral-corrugated nozzle with a twisted tape installed. Thermophysics and Aeromechanics, 29(4): 519-530. https://doi.org/10.1134/S0869864322040059

[11] Das, S., Verma, N., Pathak, M., Bhattacharyya, S. (2021). Axially oriented structured porous layers for heat transfer enhancement in a solar receiver tube. Journal of Thermal Science, 30(5): 1643-1657. https://doi.org/10.1007/s11630-021-1514-4

[12] Han, S.F., Fan, X. (1992). An investigation on internal thermal flow of non-Newtonian fluid. Applied Mathematics and Mechanics, 13(5): 425-435. https://doi.org/10.1007/BF02450733

[13] Ahamed, J.U., Wazed, M.A., Ahmed, S., Nukman, Y., Ya, T.T., Sarkar, M.A.R. (2011). Enhancement and prediction of heat transfer rate in turbulent flow through tube with perforated twisted tape inserts: A new correlation. ASME Journal of Heat and Mass Transfer, 133(4): 041903. https://doi.org/10.1115/1.4002635

[14] Salam, B., Biswas, S., Saha, S., Bhuiya, M. M.K. (2013). Heat transfer enhancement in a tube using rectangular-cut twisted tape insert. Procedia Engineering, 56: 96-103.

https://doi.org/10.1016/j.proeng.2013.03.094
[15] Hossain, S., Deb, U.K., Rahman, K.A. (2015). The enhancement of heat transfer in a circular tube with insert and without insert by using the finite element method. Procedia Engineering, 105: 81-88. https://doi.org/10.1016/j.proeng.2015.05.010
[16] Acherjee, S., Deb, U.K., Bhuyan, M.M. (2020). The effect of the angle of perforation on perforated inserts in a pipe flow for heat transfer analysis. Mathematics and Computers in Simulation, 171: 306-314. https://doi.org/10.1016/j.matcom.2019.10.003
[17] Chowdhury, M.K., Bhuyan, M.M., Deb, U.K. (2019). Augmentation of heat transfer in pipe flow using plain twisted tape inserts for different twist ratios. Energy and Power Engineering, 11(9): 342-354. https://doi.org/10.4236/epe.2019.119022
[18] Nashee, S.R. (2023). Numerical study for fluid flow and Heat transfer characteristics in a corrugating channel. International Journal of Heat & Technology, 41(2): 392-398. https://doi.org/10.18280/ijht.410213
[19] Nashee, S.R., Ibrahim, Z.A., Kamil, D.J. (2024). Numerical investigation of flow in vertical rectangular channels equipped with three different obstacles shape. AIP Conference Proceeding, 3122(1): 100002. https://doi.org/10.1063/5.0216016
[20] Shakir, R. (2023). Prediction study of the boiling flow of heat transfer in an array of in-line micro-pin-fins heat sink. American Institute of Physics Conference Series, 2845(1): 060003. https://doi.org/10.1063/5.0157017
[21] Hamood, H.M., Mansour, M.M., Lafta, A.M., Nashee, S.R. (2024). Numerical investigation to study the effect of three height of triangular obstacles on heat transfer of nanofluids in a microchannel. International Review of Mechanical Engineering, 17(11): 533. https://doi.org/10.15866/ireme.v17i11.23627
[22] Nashee, S.R. (2024). Numerical Simulation of Heat Transfer Enhancement of a Heat Exchanger Tube Fitted with Single and Double-Cut Twisted tapes. International Journal of Heat and Technology, 42(3): 1003-1010. https://doi.org/10.18280/ijht.420327
[23] Reddy, J.N. (2005). An Introduction to the Finite Element Method (Vol. 3). New York: McGraw-Hill.
[24] www.comsolmultiphysics.com, accessed on June 20, 2024.
[25] Menter, F.R. (1994). Two-equation eddy-viscosity turbulence models for engineering applications. AIAA Journal, 32(8): 1598-1605. https://doi.org/10.2514/3.12149
[26] Wilcox, D.C. (1994). Simulation of transition with a two-equation turbulence model. AIAA Journal, 32(2): 247-255. https://doi.org/10.2514/3.59994
[27] Bhuiya, M.M.K., Ahamed, J.U., Sarkar, M.A.R., Salam, B., Sayem, A.S.M., Rahman, A. (2014). Performance of turbulent flow heat transfer through a tube with perforated strip inserts. Heat Transfer Engineering, 35(1): 43-52. https://doi.org/10.1080/01457632.2013.810449
[28] Bhuiya, M.M.K., Chowdhury, M.S.U., Islam, M., Ahamed, J.U., Khan, M.J.H., Sarker, M.R.I., Saha, M. (2012). Heat transfer performance evaluation for turbulent flow through a tube with twisted wire brush inserts. International Communications in Heat and Mass Transfer, 39(10): 1505-1512. https://doi.org/10.1016/j.icheatmasstransfer.2012.10.005
[29] Eiamsa-Ard, S., Thianpong, C., Eiamsa-Ard, P., Promvonge, P. (2009). Convective heat transfer in a circular tube with short-length twisted tape insert. International Communications in Heat and Mass Transfer, 36(4): 365-371. https://doi.org/10.1016/j.icheatmasstransfer.2009.01.006
[30] Acherjee, S., Shahriar, M., Bhuyan, M.M., Deb, U.K. (2017). Enhancement of heat transfer in a u-loop circular tube with axial perforated inserts. Southeast Asian Journal of Sciences, 5(2): 126-136.
[31] Bhuyan, M.M., Deb, U.K., Shahriar, M., Acherjee, S. (2017). Simulation of heat transfer in a tubular U-loop pipe using the rectangular inserts and without insert. AIP Conference Proceedings, 1851(1): 020011. http://doi.org/10.1063/1.4984640
[32] Eiamsa-Ard, P., Piriyarungroj, N., Thianpong, C., Eiamsa-Ard, S. (2014). A case study on thermal performance assessment of a heat exchanger tube equipped with regularly-spaced twisted tapes as swirl generators. Case Studies in Thermal Engineering, 3: 86-102. http://doi.org/10.1016/j.csite.2014.04.002
[33] Piriyarungrod, N., Eiamsa-Ard, S., Thianpong, C., Pimsarn, M., Nanan, K.J.C.E. (2015). Heat transfer enhancement by tapered twisted tape inserts. Chemical Engineering and Processing: Process Intensification, 96: 62-71. http://doi.org/10.1016/j.cep.2015.08.002
[34] Rahimi, M., Shabanian, S.R., Alsairafi, A.A. (2009). Experimental and CFD studies on heat transfer and friction factor characteristics of a tube equipped with modified twisted tape inserts. Chemical Engineering and Processing: Process Intensification, 48(3): 762-770. http://doi.org/10.1016/j.cep.2008.09.007
[35] Chang, S.W., Jan, Y.J., Liou, J.S. (2007). Turbulent heat transfer and pressure drop in tube fitted with serrated twisted tape. International Journal of Thermal Sciences, 46(5): 506-518. http://doi:10.1016/j.ijthermalsci.2006.07.009

NOMENCLATURE

l	length of the pipe
D	diameter of the pipe
C_P	specific heat, J. kg^{-1}. K^{-1}
ΔP	pressure drop
g	gravitational acceleration, m.s^{-2}
k	thermal conductivity, W.m^{-1}. K^{-1}
f	friction factor(-)
Nu	Nusselt number(-)
Re	Reynolds number(-)
Ti	inlet temperature (K)
To	outlet temperature (K)
Tb	bulk temperature (K)
Tw	wall temperature (K)
$Twav$	average wall temperature (K)
q	heat flux (W/m^2)
Q	amount of heat Joule(j)

Greek symbols

μ	dynamic viscosity, kg. m^{-1}.s^{-1}
ω	inverse time scale
μ_T	turbulent viscosity

ε	effectiveness
η	thermal enhancement performance
ρ	density of water

Subscripts

p	plain tube
t	twisted tape